



**HAL**  
open science

## Preparation and characterization of $\text{Pr}_2\text{NiO}_{4+\delta}$ infiltrated into Gd-doped ceria as SOFC cathode

Clément Nicollet, Aurélien Flura, Vaibhav Vibhu, Sébastien Fourcade, Aline Rougier, Jean-Marc. Bassat, Jean-Claude Grenier

### ► To cite this version:

Clément Nicollet, Aurélien Flura, Vaibhav Vibhu, Sébastien Fourcade, Aline Rougier, et al.. Preparation and characterization of  $\text{Pr}_2\text{NiO}_{4+\delta}$  infiltrated into Gd-doped ceria as SOFC cathode. *Journal of Solid State Electrochemistry*, 2016, 20 (7), pp.2071-2078. 10.1007/s10008-016-3211-x . hal-01338305

**HAL Id: hal-01338305**

**<https://hal.science/hal-01338305>**

Submitted on 18 Jan 2021

**HAL** is a multi-disciplinary open access archive for the deposit and dissemination of scientific research documents, whether they are published or not. The documents may come from teaching and research institutions in France or abroad, or from public or private research centers.

L'archive ouverte pluridisciplinaire **HAL**, est destinée au dépôt et à la diffusion de documents scientifiques de niveau recherche, publiés ou non, émanant des établissements d'enseignement et de recherche français ou étrangers, des laboratoires publics ou privés.

# Preparation and characterization of $\text{Pr}_2\text{NiO}_{4+\delta}$ infiltrated into Gd-doped ceria as SOFC cathode

Clément Nicollet<sup>1</sup> · Aurélien Flura<sup>1</sup> · Vaibhav Vibhu<sup>1</sup> · Sébastien Fourcade<sup>1</sup> · Aline Rougier<sup>1</sup> · Jean-Marc Bassat<sup>1</sup> · Jean-Claude Grenier<sup>1</sup>

**Abstract** Composite electrodes of  $\text{Pr}_2\text{NiO}_{4+\delta}$  and Gd-doped ceria ( $\text{Ce}_{0.8}\text{Gd}_{0.2}\text{O}_{1.90}$  so-called GDC) have been prepared starting from a Pr-Ni nitrate solution (2:1 stoichiometry ratio) that was infiltrated into a porous GDC backbone made by screen printing onto 3 % yttria-stabilized zirconia membrane (90  $\mu\text{m}$  thick). The crystallization of the  $\text{Pr}_2\text{NiO}_{4+\delta}$  powder was first studied by X-ray diffraction: it highly depends on the annealing atmosphere (air or  $\text{N}_2$ ) and the formation of this phase as infiltrate is more difficult than for the powder. The electrochemical study performed on symmetrical cells shows that the polarization resistance decreases when the annealing temperature of the infiltrate electrode decreases. The lowest  $R_p$  value is obtained for an annealing at 900 °C, for 2 h in  $\text{N}_2$ , the value being 0.075  $\Omega \text{ cm}^2$  at 600 °C in air.

**Keywords** SOFC composite cathode · Praseodymium nickelate · Infiltration process · Electrochemical impedance spectroscopy · ALS model

## Introduction

Among possible candidates as cathode for solid oxide fuel cells operating at intermediate temperatures, a keen interest has grown in the community regarding the Ruddlesden-

Popper phases  $\text{Ln}_2\text{NiO}_{4+\delta}$  ( $\text{Ln} = \text{La}, \text{Pr}, \text{Nd}$ ) [1–3] thanks to high values of both surface exchange ( $k$ ) and oxygen diffusion coefficients ( $D_{\text{O}^2}$ ) [4]. More particularly,  $\text{Pr}_2\text{NiO}_{4+\delta}$  exhibits the highest values and its use as SOFC oxygen electrode leads to polarization resistance as low as that of the reference material  $\text{La}_{0.6}\text{Sr}_{0.4}\text{Fe}_{0.8}\text{Co}_{0.2}\text{O}_{3-\delta}$  [5, 6].

The most usual way to produce efficient SOFC cathodes is the screen-printing deposition technique, which allows obtaining a uniform porous layer of the electrode material onto the electrolyte substrate. Then, this layer has to be sintered at high temperature to insure a good adherence to the substrate as well as connection between grains. Although this low cost technique is widely used to produce commercial SOFC electrodes, the required high-sintering temperatures may cause various problems such as reactivity between the electrolyte and the electrode, e.g., formation of detrimental interphases [7].

Such inter-diffusion issues are even more pronounced in the case of composite electrodes because the electrolyte and electrode materials are intimately mixed together. However, for these electrodes, an alternative fabrication process has recently received significant attention, namely the infiltration of the catalyst material into a highly porous backbone [8–10]. With this technique, only the backbone is deposited by screen printing and sintered at high temperature, while the catalyst is infiltrated into the porous backbone and generally annealed at lower temperature. When the backbone is of the same nature or chemically compatible with the electrolyte, high processing temperatures are not a problem anymore, so the mechanical strength of the electrode can easily be achieved. As the catalyst is usually infiltrated starting from solutions, it forms a fine nano-scaled catalyst network uniformly covering the backbone that can be preserved after annealing at rather low temperature (600–1000 °C).

As a matter of fact, this technique allows making very efficient electrodes for oxygen reduction: Samson et al. [11]

---

**Electronic supplementary material** The online version of this article (doi:10.1007/s10008-016-3211-x) contains supplementary material, which is available to authorized users.

---

✉ Jean Claude Grenier  
Jean.Claude.Grenier@icmcb.cnrs.fr

<sup>1</sup> ICMCB, CNRS, Université Bordeaux, 87 Av. Dr Schweitzer, 33608 Pessac, France

reported for  $\text{La}_{0.6}\text{Sr}_{0.4}\text{CoO}_{3-\delta}$  infiltrated into Gd-doped ceria (so-called GDC) a polarization resistance,  $R_p = 0.044 \Omega \text{ cm}^2$  at 600 °C. Concerning the nickelate materials, Nicollet et al. [12] obtained for  $\text{La}_2\text{NiO}_{4+\delta}$  infiltrated into GDC, a polarization resistance value as low as  $0.15 \Omega \text{ cm}^2$  at 600 °C. Recently,  $\text{Pr}_2\text{NiO}_{4+\delta}$  was used by Railsback et al. [13] as the catalyst of an infiltrated electrode with  $\text{La}_{0.9}\text{Sr}_{0.1}\text{Ga}_{0.8}\text{Mg}_{0.2}\text{O}_{3-\delta}$  as backbone; they measured a  $R_p$  value of  $0.11 \Omega \text{ cm}^2$  at 650 °C. These authors also evidenced that  $\text{Pr}_2\text{NiO}_{4+\delta}$  is chemically stable as an infiltrate, even though the phase is known to decompose at operating temperatures (600–800 °C), as shown by Kovalesky et al. [14].

As the strontium is known to react with chromium species coming from steel interconnects and form  $\text{SrCrO}_4$  [15], a strontium-free electrode is highly desirable to prevent the decrease of the cell performance. In this work, the Gd-doped ceria that has a slightly higher ionic conductivity than  $\text{La}_{0.9}\text{Sr}_{0.1}\text{Ga}_{0.8}\text{Mn}_{0.2}\text{O}_{3-\delta}$ , is used as the ionic conducting backbone and is infiltrated with  $\text{Pr}_2\text{NiO}_{4+\delta}$ . In a first part, the crystallization of  $\text{Pr}_2\text{NiO}_{4+\delta}$  is studied starting from nitrate solution ( $\text{Pr}/\text{Ni} = 2$ ) fired and annealed in different atmospheres (air and nitrogen). Then, on the basis of these results, electrodes of infiltrated Pr/Ni solution into Gd-doped backbones are prepared. Finally, their electrochemical properties are measured by impedance spectroscopy in a symmetrical cell and compared with those of classical screen-printed electrode of  $\text{Pr}_2\text{NiO}_{4+\delta}$  to characterize the benefits of the infiltration technique.

## Experimental

### Cell fabrication

The symmetrical cells were made with commercial 3 wt.% yttria-stabilized zirconia, 3YSZ, membranes of  $\varnothing = 25 \text{ mm}$  and a thickness of 90  $\mu\text{m}$  (kindly provided by ECN, The Netherlands), on which a porous GDC backbone ( $\varnothing = 15 \text{ mm}$ ,  $\approx 8 \mu\text{m}$  thick) and a  $\text{LaNi}_{0.6}\text{Fe}_{0.4}\text{O}_{3-\delta}$  (LNF) collecting layer ( $\approx 10 \mu\text{m}$  thick) were successively deposited by screen printing, both being fired at 1150 °C for 1 h in air. The backbone and LNF layer were infiltrated with a Pr and Ni nitrate solution with a molar ratio of 2:1, and calcined at 450 °C for 20 min, in air. The calcined infiltrate will be referred as Pr2:Ni in the paper, keeping in mind that the molar ratio is always 2. A more detailed explanation of the infiltration process is described elsewhere [12]. The infiltration step is repeated until the mass ratio of the infiltrated material over the backbone reaches about 30 wt.%. The cells were then annealed following heat treatments described below. In addition, it has been controlled that the GDC backbone is thick enough so that the diffusion length does not extend to the LNF layer, that only acts as a current collector and takes no part in the electrochemical response of the electrode.

For the screen-printed  $\text{Pr}_2\text{NiO}_{4+\delta}$  symmetrical cells, a GDC ink was prepared from commercial powder (Rhodia) and first screen printed on the electrolyte, then sintered at 1300 °C for 1 h to form a 1- $\mu\text{m}$  thick barrier layer. The  $\text{Pr}_2\text{NiO}_{4+\delta}$  electrode was also prepared by screen printing an ink made of a commercial powder (Marion technologies) and sintered at 1150 °C for 1 h to form a 10- $\mu\text{m}$  thick layer. A collecting layer is not necessary as  $\text{Pr}_2\text{NiO}_{4+\delta}$  has a good electronic conductivity.

### X-ray diffraction analyses

X-ray diffractograms were recorded on a PANalytical X'pert MPD-pro diffractometer of Bragg-Brentano geometry using the  $K\alpha$  emission of a Cu source.

### Thermogravimetry analysis

Thermogravimetry analyses (TGA) were carried out using a TA Instrument TGA-Q50 device.

### SEM analysis

The SEM images were recorded with a field emission scanning electron microscope Jeol JSM 6700 F at an acceleration voltage of 1 kV. Samples were fractured and the images were taken on the cross section. Prior to analysis, the samples were sputtered with palladium to avoid electron charging.

### Electrochemical measurements

Measurements on the symmetrical cells were carried out in a setup where the sample is placed between two designed ceramics mounted with gold grids for the current collection. The channeled ceramics provide an efficient distribution of air to the electrodes leading to minimize the gas diffusion impedance [16]. A weight is applied to improve the current collection of the gold grids. The impedance diagrams are recorded with a Solartron Modulab frequency response analyzer from 1 to 10 mHz. The data are fitted using Zview software (Scribner®) to determine the polarization resistance of the electrode. The good quality of each measurement is controlled with the Kramers-Kronig transformation using an in-house software (CANELEIS®).

## Results and discussion

### Preliminary experiments: phase formation

To determine the temperature at which the  $\text{Pr}_2\text{NiO}_{4+\delta}$  phase forms, the Pr2:Ni nitrate solution was burnt at 450 °C and heated at various temperatures, in air or  $\text{N}_2$  atmospheres, the

resulting powder being characterized by X-ray diffraction. Figure 1a shows the X-ray diffraction patterns of the powders sintered in air, at temperature ranging from 600 °C to 1000 °C, for 2 h. From 600 to 900 °C, the  $\text{Pr}_2\text{NiO}_{4+\delta}$  phase does not seem to form and only the X-ray diffraction peaks of the two simple oxides  $\text{Pr}_6\text{O}_{11}$  and NiO are visible. Their intensity increases and the full width at half maximum (FWHM) decreases as the sintering temperature increases, i.e., as the crystallite size increases. The  $\text{Pr}_2\text{NiO}_{4+\delta}$  phase starts to crystallize only when the nitrate mixture is fired at 1000 °C; however, the sintering duration is not long enough to obtain the pure  $\text{Pr}_2\text{NiO}_{4+\delta}$  phase, some amount of  $\text{Pr}_6\text{O}_{11}$  and NiO remains. In a recent work, Railsback et al. [13] observed the same tendency and found that  $\text{Pr}_6\text{O}_{11}$  was still present even after a heat treatment at 1100 °C for 4 h. Such a high temperature would be harsh to apply to an infiltrated electrode, as it will

strongly favor the inter-diffusion between the Pr2:Ni infiltrate and the GDC backbone or the YSZ electrolyte.

Thermal treatment under  $\text{N}_2$  atmosphere, i.e., at lower oxygen partial pressure,  $p\text{O}_2 \approx 5.10^{-4}$  atm, leads to form the  $\text{Pr}_2\text{NiO}_{4+\delta}$  phase at lower temperature than in air. Figure 1b shows the X-ray diffractograms of the same powder obtained from calcined nitrates, sintered at 800 and 900 °C for 2 h in  $\text{N}_2$  atmosphere. The  $\text{Pr}_2\text{NiO}_{4+\delta}$  phase starts to form at about 800 °C, i.e., 200 °C lower than in air, but the  $\text{Pr}_6\text{O}_{11}$  and NiO phases are still present. Longer treatment at this temperature would be needed to produce pure  $\text{Pr}_2\text{NiO}_{4+\delta}$  powder. After thermal treatment at 900 °C, for 2 h, the  $\text{Pr}_2\text{NiO}_{4+\delta}$  phase is fully formed (Fig. 1b). The benefit of heat treatment in  $\text{N}_2$  could come from the valence of Pr in the starting powder. In  $\text{Pr}_6\text{O}_{11}$ , Pr has a mixed 3+/4+ valence, whereas in  $\text{Pr}_2\text{NiO}_{4+\delta}$  only trivalent Pr is present [17]. Figure 2 shows the

**Fig. 1** X ray diffractograms of fired Pr2:Ni nitrate solutions after annealing at various temperatures for 2 h in air (a) or  $\text{N}_2$  atmospheres (b)

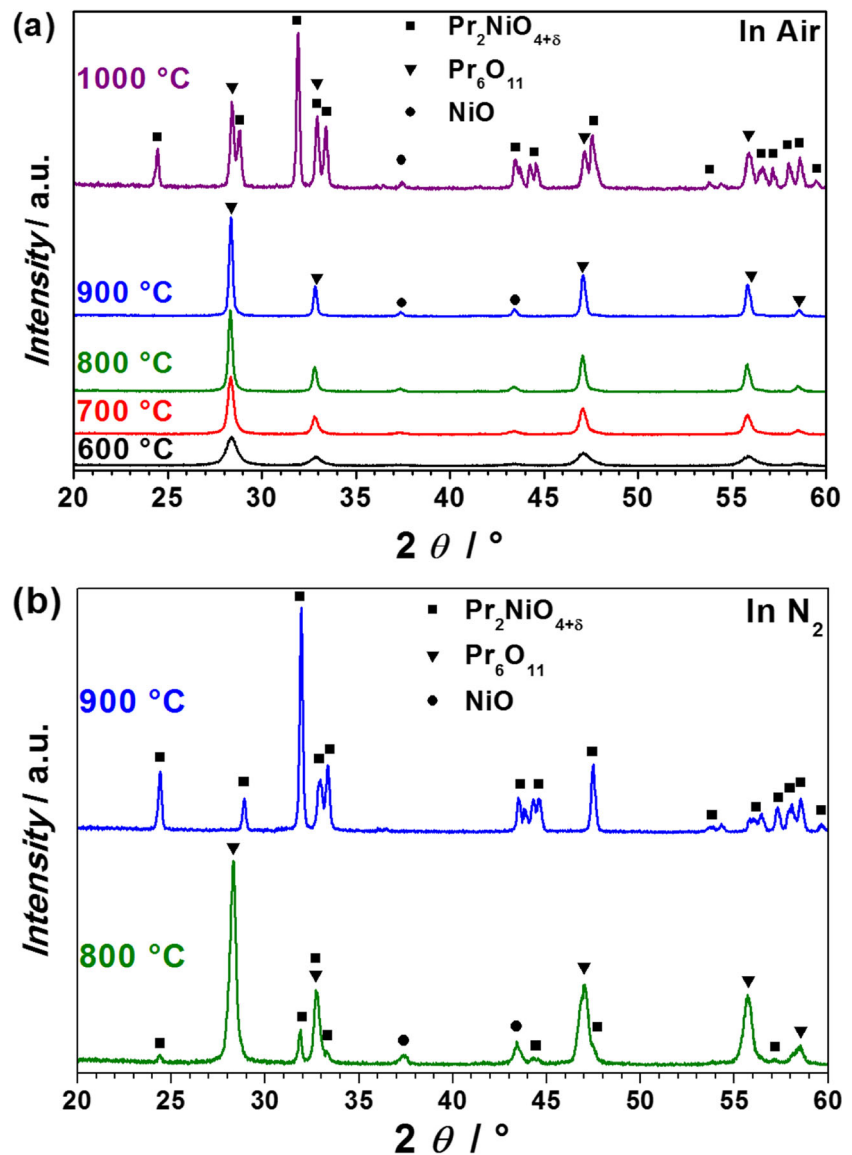
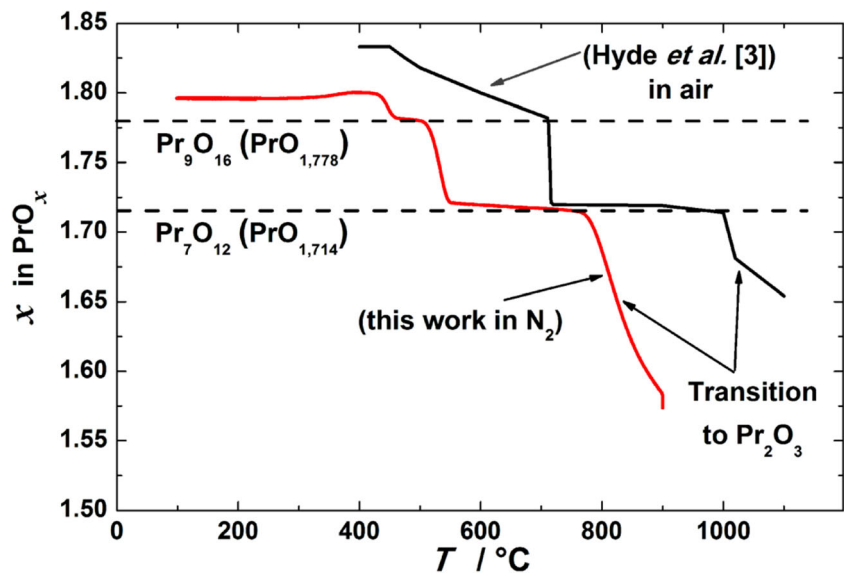


**Fig. 2** Thermogravimetric analyses of praseodymium oxide carried out in air by Hyde et al. [17] and in N<sub>2</sub> atmosphere (this work)



thermogravimetric analyses of Pr<sub>6</sub>O<sub>11</sub> in air (carried out by Hyde et al. [18]) and, for comparison, in N<sub>2</sub> gas (this work). In air, upon heating up to 1000 °C, Pr<sub>6</sub>O<sub>11</sub> undergoes a first phase transition at around 700 °C to form Pr<sub>7</sub>O<sub>12</sub>, which also exhibits a mixed 3+/4+ valence for Pr, and a second transition at around 1000 °C leading to Pr<sub>2</sub>O<sub>3</sub> with only Pr<sup>3+</sup>. At lower oxygen partial pressure (typically in N<sub>2</sub> atmosphere), the Pr<sub>6</sub>O<sub>11</sub>/Pr<sub>7</sub>O<sub>12</sub> and Pr<sub>7</sub>O<sub>12</sub>/Pr<sub>2</sub>O<sub>3</sub> transitions are shifted to lower temperatures, namely 500 °C, and 800–900 °C (Fig. 2). In both atmospheres, the temperatures of formation of Pr<sub>2</sub>O<sub>3</sub> match well with those of Pr<sub>2</sub>NiO<sub>4+δ</sub> (Fig. 1). Such features indicate that the presence of Pr<sup>4+</sup> somehow inhibits the formation of Pr<sub>2</sub>NiO<sub>4+δ</sub>, which only starts to form when the valence of the Pr precursors matches its own, i.e., 3+ only.

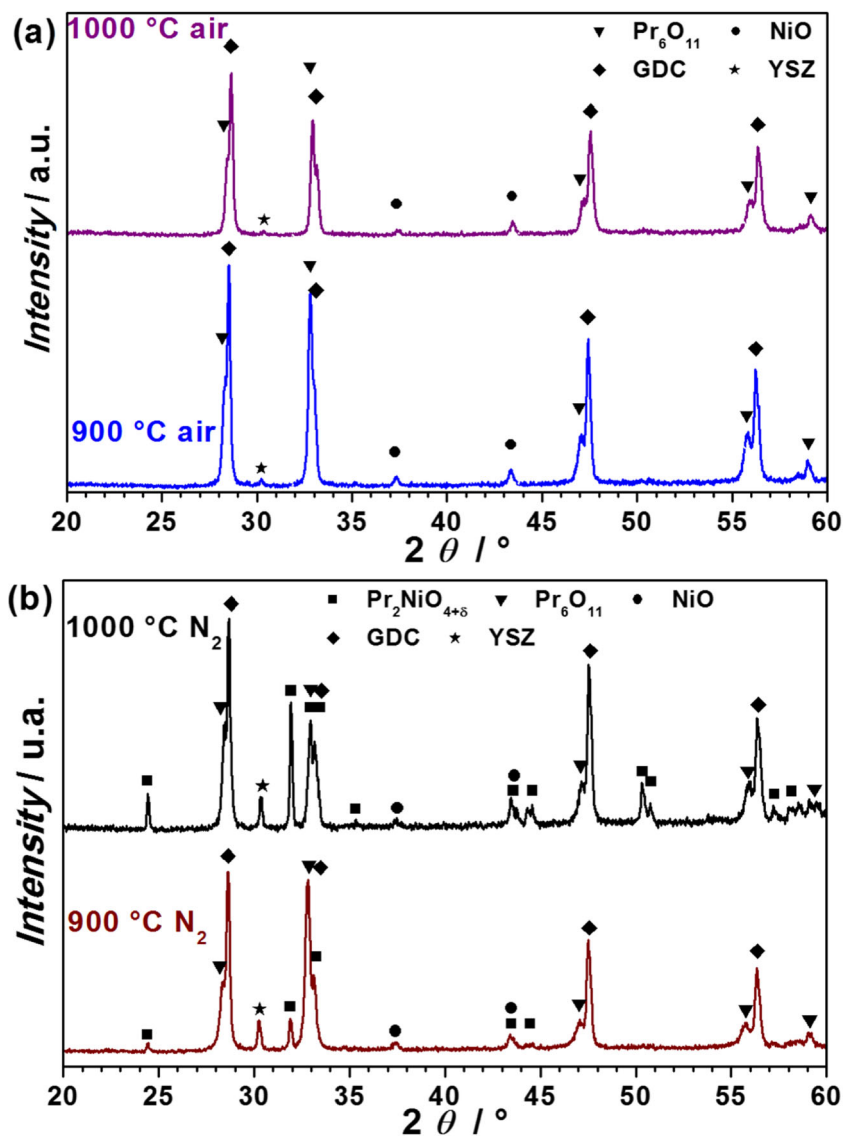
### Characterization of infiltrated electrodes

On the basis of the previous results, infiltration experiments of Pr<sub>2</sub>:Ni nitrate solutions into the GDC backbones were carried out. Figure 3 shows the X-ray diffractograms of four Pr<sub>2</sub>:Ni infiltrated electrodes annealed either at 900 or 1000 °C, for 2 h under air or N<sub>2</sub>. Surprisingly, in air (Fig. 3a), the Pr<sub>2</sub>NiO<sub>4+δ</sub> phase is not evidenced, even at 1000 °C. One should point out that at this temperature Railsback et al. obtained Pr<sub>2</sub>NiO<sub>4+δ</sub> infiltrated in a La<sub>0.9</sub>Sr<sub>0.1</sub>Ga<sub>0.8</sub>Mg<sub>0.2</sub>O<sub>3-δ</sub> (LSGM) backbone [13], which would mean that the nature of the backbone has some influence on the formation of the infiltrated phase. Indeed, they proposed that La diffusion from the LSGM backbone into the infiltrated phase could stabilize the phase and favor its formation. In this study, the Gd-doped ceria backbone is a fluorite-type phase, isostructural to Pr<sub>6</sub>O<sub>11</sub> present after the calcination at 450 °C, which might result in the stabilization of Pr<sub>6</sub>O<sub>11</sub> through an epitaxial process, inhibiting the formation of Pr<sub>2</sub>NiO<sub>4+δ</sub>.

The thermal treatment in N<sub>2</sub> atmosphere (Fig. 3b) at 900 °C, for 2 h, leads to form Pr<sub>2</sub>NiO<sub>4+δ</sub>, however not as a pure phase as obtained in the case of powder samples, a significant amount of Pr<sub>6</sub>O<sub>11</sub> still remaining. It is noteworthy that an annealing for 6 h did not significantly increase the proportion of Pr<sub>2</sub>NiO<sub>4+δ</sub>, which would mean that the phase formation is not kinetically controlled and 2 h treatments are enough to reach a steady state. At 1000 °C, for 2 h in N<sub>2</sub>, Pr<sub>2</sub>NiO<sub>4+δ</sub> is the major phase, despite the presence of some amount of Pr<sub>6</sub>O<sub>11</sub>. Sintering at higher temperatures is not recommended as the specific surface area of the electrode would decrease and the reactivity between the Pr<sub>2</sub>:Ni infiltrated phase, GDC backbone, and the YSZ electrolyte would dramatically increase. Sintering at lower temperatures is not significant as Pr<sub>2</sub>NiO<sub>4+δ</sub> is not formed.

Figure 4 shows SEM images of an infiltrated electrode. Figure 4a corresponds to a global view of the infiltrated electrode annealed at 1000 °C, which allows measuring the thicknesses of both GDC backbone and LNF collecting layer. They are typically around 8 μm for GDC and 10 μm for LNF. Figure 4b shows the microstructure of the GDC backbone prior to infiltration: the average grain size of GDC is around 200 nm. Figure 4c shows the microstructure of the infiltrated GDC annealed at 900 °C for 2 h in N<sub>2</sub>. The infiltrated phase entirely covers the GDC grains, and the annealing treatment sintered the infiltrated phase, as grain boundaries can be distinguished (which are not seen on the GDC backbone alone). In addition, nanoparticles of the infiltrated phase (40–80 nm) also are formed. These nanoparticles are no longer present after an annealing treatment at 1000 °C. As the annealing temperature increases, the infiltrated phase is further sintered, which certainly has an important effect on the specific surface area of the electrode.

**Fig. 3** X ray diffractograms of Pr<sub>2</sub>:Ni solution infiltrated into Gd doped ceria backbones annealed at 900 and 1000 °C for 2 h in air (a) and in N<sub>2</sub> gas (b)



### EIS measurements on symmetrical cells

Two symmetrical cells with electrodes of Pr<sub>2</sub>:Ni infiltrated into a GDC backbone were prepared, the first one annealed at 900 °C and the other one at 1000 °C, both for 2 h in N<sub>2</sub> atmosphere. The cell annealed at 900 °C was also considered for impedance measurements as an annealing at lower temperature may provide a higher specific surface area.

In addition, the EIS response of the LNF current collector was measured (Online resource 1). With regard to the high values of the polarization resistances (for instance,  $R_p \approx 47 \Omega \text{ cm}^2$  at 600 °C), it can be concluded that this conducting layer will not take part into the electrochemical response of the electrode.

Figure 5 shows the Nyquist and Bode plots recorded at 400 and 600 °C for both symmetrical cells. Two contributions (P1 and P2) are visible in the impedance

diagrams at 400 °C and three (P1, P2, and P3) at 600 °C. Actually, the P3 contribution occurring only at high temperature is assigned to the diffusion of gaseous O<sub>2</sub> to the active sites of the electrode. It has been shown that this small contribution (around 14 mΩ cm<sup>2</sup>) is mostly related to the impedance measurement setup [16] and occurs only at high temperatures because it is not overlapped by the P2 contribution. The P3 contribution has been fitted with a finite length Warburg impedance and will not be discussed any further as it is beyond the scope of this study.

The P1 and P2 contributions were fitted using R//CPE elements to calculate their respective polarization resistances. A series resistance was added to the equivalent circuit to model the electrolyte resistance, as well as an inductance at 550 and 600 °C to take into account the impedance of wires that deforms the P1 contribution.

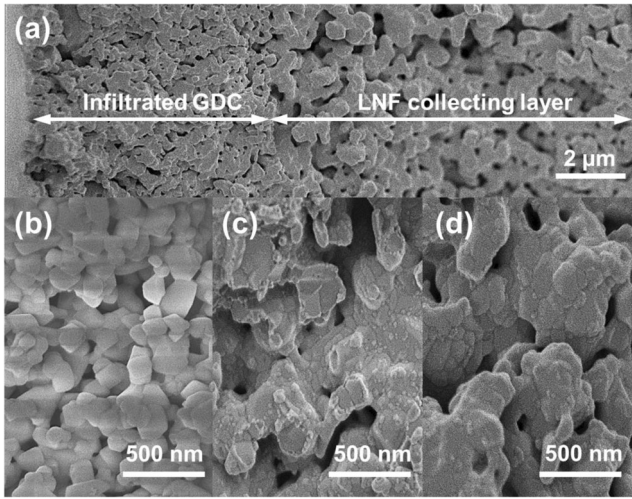


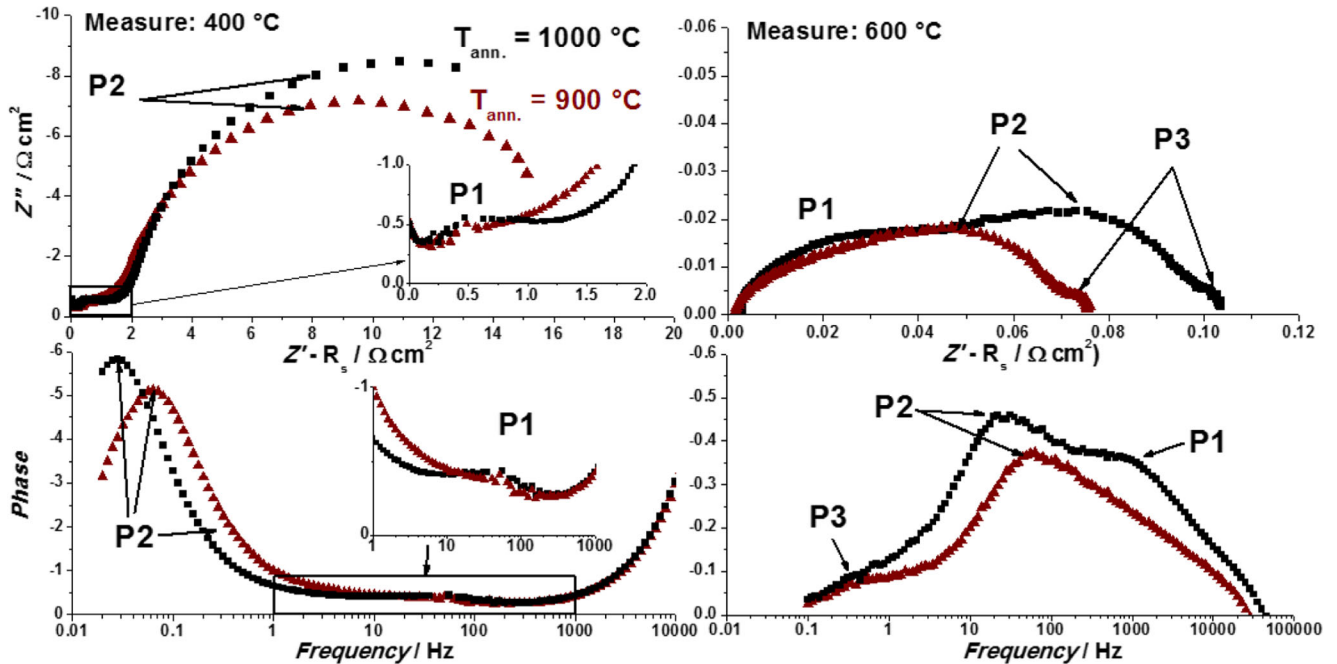
**Fig. 4** SEM cross section images of the infiltrated electrode annealed at 1000 °C for 2 h in N<sub>2</sub> (a, d), of the GDC backbone prior to infiltration (b), and of the GDC backbone infiltrated with Pr<sub>2</sub>:Ni annealed at 900 °C for 2 h in N<sub>2</sub> (c)

The capacitances corresponding to the P1 contribution (at 400 and 600 °C) are around  $C \approx 10^{-2} \text{ F cm}^{-2}$ , meaning that P1 cannot be related to a double layer capacitance occurring at the electrolyte electrode interface (the values being usually around  $10^{-4}$ – $10^{-6} \text{ F cm}^{-2}$ ). It is rather related to a polarization resistance due to the oxide ion diffusion through an interphase created during the annealing treatment. Indeed, a recent study has shown that modification of the electrode/electrolyte interface can create or

suppress additional contributions [19]. Further analyses would be required to confirm this hypothesis. The contribution P2 is assigned to the oxygen electrode reaction (OER) related to Pr<sub>2</sub>NiO<sub>4+δ</sub>, since its relaxation times (and related capacitances  $\approx 0.2 \text{ F cm}^{-2}$ ) are consistent with previous results obtained on conventional Pr<sub>2</sub>NiO<sub>4+δ</sub>/GDC/Pr<sub>2</sub>NiO<sub>4+δ</sub> symmetrical cells [6].

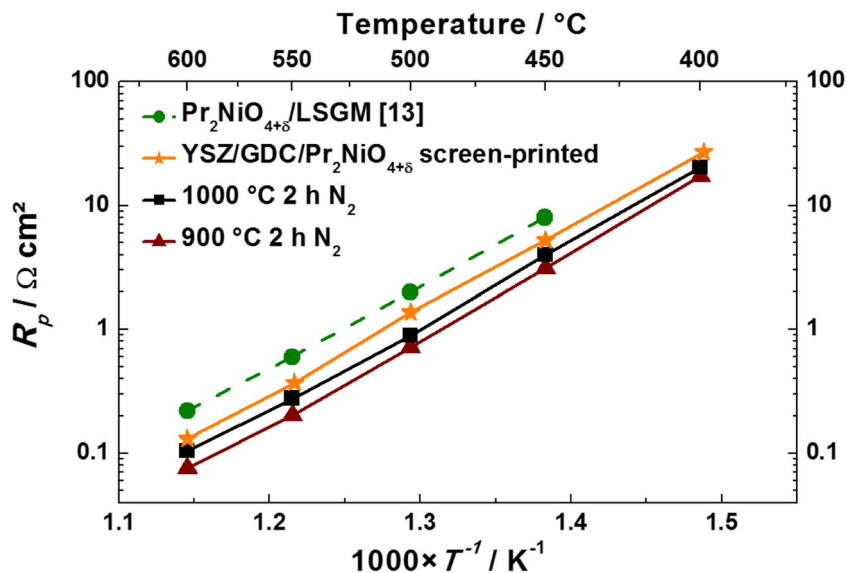
Figure 5 shows a decrease of P2 relaxation frequency when increasing the annealing temperature. This evolution can be analyzed on the basis of the Adler-Lane-Steel model that correlates  $R_{\text{chem}}$ , the chemical resistance and  $t_{\text{chem}}$ , the chemical time constant related to the OER, to the microstructure of the electrode [20]. In particular, both parameters being inversely proportional to the specific surface area, it results that the relaxation frequency,  $f_{\text{relaxation}} = 1/(2\pi \cdot t_{\text{chem}})$ , is proportional to the specific surface area. Increasing the annealing temperature likely results in the coarsening of infiltrated particles, leading to a decrease of the specific surface area of the electrode. Such an evolution would be consistent with the increase of the relaxation time of P2 with the electrode annealing temperature.

Figure 6 shows the thermal variation of  $R_p$  in the range 400–600 °C, calculated by adding the polarization resistances related to the three processes P1, P2, and P3, and compared with the values obtained with a screen-printed Pr<sub>2</sub>NiO<sub>4+δ</sub> electrode on a YSZ electrolyte with a GDC barrier layer. The results of Railsback et al. [13] on Pr<sub>2</sub>NiO<sub>4+δ</sub> infiltrated into LSGM are also added.



**Fig. 5** Nyquist and Bode plots of the impedance measurements recorded in air at 400 and 600 °C for symmetrical cells (Pr<sub>2</sub>NiO<sub>4+δ</sub>/GDC//3YSZ//Pr<sub>2</sub>NiO<sub>4+δ</sub>/GDC) annealed at 900 and 1000 °C for 2 h in N<sub>2</sub> atmosphere

**Fig. 6** Arrhenius plots of the  $R_p$  for symmetrical cells annealed at 900 and 1000 °C for 2 h in  $N_2$  atmosphere compared with those of a screen printed electrode and of results of reference [13]



Both infiltrated cells have lower polarization resistances than that of a screen-printed  $Pr_2NiO_{4+\delta}$  electrode measured in the same conditions. Furthermore, the polarization resistances are lower than that of  $Pr_2NiO_{4+\delta}/LSGM$  infiltrated electrode that was annealed at 1000 °C in air, yielding pure  $Pr_2NiO_{4+\delta}$  [13]. The authors suggest that the La or Ga from the LSGM backbone could diffuse in the infiltrated phase. Recently, Vibhu et al. [21] showed that the substitution of La for Pr in  $Pr_2NiO_{4+\delta}$  leads to a more stable phase, which would explain why these authors obtained a pure phase (probably La doped) at 1000 °C in air, unlike the results of this present study. Additionally, Vibhu et al. showed that the polarization resistance increases with the fraction of La in the phase. This effect, along with the ionic conductivity of GDC being a little bit higher than that of LSGM, could explain why our cells show lower polarization resistances.

Although the cell annealed at 1000 °C for 2 h in  $N_2$  exhibits the largest amount of  $Pr_2NiO_{4+\delta}$  phase, the value of  $R_p$  is slightly lower for the cell annealed at 900 °C over the whole temperature range, reaching  $0.075 \Omega \text{ cm}^2$  at 600 °C. One can suggest two hypotheses to explain the slightly smaller values. First, one can assume that low annealing temperatures result in larger specific surface area of the electrocatalyst (as previously suggested [11]), which improves the solid/gas exchange reaction, leading to lower the  $R_p$  values. Secondly, the presence of the residual phase,  $Pr_6O_{11}$ , might actually improve the cell performance. Indeed, few authors have already reported that decorating an electrode surface with  $Pr_6O_{11}$  improves the solid-gas reaction and leads to a decrease of the polarization resistance [22–24], suggesting that it has interesting catalytic properties. Here, the association of the ionic and electronic conductivities of  $Pr_2NiO_{4+\delta}$  and the catalytic activity of  $Pr_6O_{11}$  could induce a decrease of the polarization resistance of the cell.

A specific study of the electrocatalytic properties of  $Pr_6O_{11}$  is in progress [25].

## Conclusion

$Pr_2NiO_{4+\delta}$  infiltrated into Gd-doped ceria electrodes have been prepared and characterized; they showed high efficiency toward the oxygen reduction reaction.

At first, it was shown that the crystallization of the  $Pr_2NiO_{4+\delta}$  phase starting from a fired Pr<sub>2</sub>:Ni nitrate solution highly depends on the atmosphere (air or  $N_2$ ) used for the last annealing treatment. The crystallization of  $Pr_2NiO_{4+\delta}$  was easier in  $N_2$  atmosphere, which seems to be correlated to the presence of  $Pr^{3+}$  in the precursors.

For infiltrated Pr<sub>2</sub>:Ni nitrate solution into Gd-doped ceria backbones, the crystallization of  $Pr_2NiO_{4+\delta}$  appeared to be more difficult and it is suggested that the Gd-doped ceria backbone inhibits the crystallization, resulting in a remaining amount of  $Pr_6O_{11}$  and NiO.

The polarization resistances determined on symmetrical cells decreased with the annealing temperature, regardless of the amount of  $Pr_2NiO_{4+\delta}$ , which could be assigned either to an increase of the specific surface area when the annealing temperature decreases, or to a beneficial synergy effect of the  $Pr_2NiO_{4+\delta}/Pr_6O_{11}$  mixture. A more detailed study of the electrocatalytic properties of  $Pr_6O_{11}$  is in progress. The lowest  $R_p$  value was obtained when the symmetrical cell was annealed at 900 °C, for 2 h in  $N_2$ , and reaches  $0.075 \Omega \text{ cm}^2$  at 600 °C.

As we recently reported for  $La_2NiO_{4+\delta}$ , the infiltration technique does represent a substantial improvement in the fabrication of SOFC electrodes with regard to the screen-printing process.

---

## References

1. Amow G, Skinner S (2006) *J Sol State Electrochem* 10(8):538–546
2. Tarancón A, Burriel M, Santiso J, Skinner S, Kilner J (2010) *J Mater Chem* 20(19):3799–3813
3. Chen Y, Zhou W, Ding D, Liu M, Ciucci F, Tade M, Shao Z (2015) *Adv Energy Mater* 5(18):1500537–1500571
4. Boehm E, Bassat JM, Dordor P, Mauvy F, Grenier JC, Stevens P (2005) *Solid State Ionics* 176:2717–2725
5. Ferchaud C, Grenier JC, Zhang Steenwinkel Y, Van Tuel M, Van Berkel F, Bassat JM (2011) *J Power Sources* 196:1872–1879
6. Philippeau B, Mauvy F, Nicollet C, Fourcade S, Grenier J (2015) *J Sol State Electrochem* 19(3):871–882
7. Adler S (2004) *Chem Rev* 104:4791–4843
8. Ding D, Li X, Lai S, Gerdes K, Liu M (2014) *Energy and Environmental Science* 7:552–575
9. Jiang S (2006) *Mater Sci Eng A* 418(1–2):199–210
10. Vohs J, Gorte R (2009) *Adv Mater* 21:943–956
11. Samson A, Søgaard M, Knibbe R, Bonanos N (2011) *J Electrochem Soc* 158:B650–B659
12. Nicollet C, Flura A, Vibhu V, Rougier A, Bassat JM, Grenier JC (2015) *J Power Sources* 294:473–482
13. Railsback JG, Gao Z, Barnett SA (2015) *Solid State Ionics* 274:134–139
14. Kovalevsky A, Kharton V, Yaremchenko A, Pivak Y, Naumovich E, Frade J (2007) *J Eur Ceram Soc* 27(13–15):4269–4272
15. Konyshva E, Penkalla H, Wessel E, Mertens J, Seeling U, Singheiser L, Hilpert K (2006) *J Electrochem Soc* 153(4):A765–A773
16. Flura A, Nicollet C, Fourcade S, Vibhu V, Rougier A, Bassat JM, Grenier JC (2015) *Electrochim Acta* 174:1030–1040
17. Ogier T (2012) Ph.D. Thesis, University of Bordeaux, #4657
18. Hyde BG, Bevan DJM, Eyring L (1966) *Mathematical and physical sciences. Phil Trans Royal Soc London*:583–614
19. Flura A, Nicollet C, Vibhu V, Zeimetz B, Rougier A, Bassat JM, Grenier JC (2016) *J Electrochem Soc* 163:F523–F532
20. Adler S, Lane J, Steele B (1996) *J Electrochem Soc* 143:3554–3564
21. Vibhu V, Rougier A, Nicollet C, Flura A, Grenier JC, Bassat JM (2015) *Solid State Ionics* 278:32–37
22. Chiba R, Aono H, Kato K (2013) *ECS Trans* 57:1831–1840
23. Ding X, Zhu W, Hua G, Li J, Wu Z (2015) *Electrochim Acta* 163:204–212
24. Navarrete L, Solis C, Serra JM (2015) *J Mater Chem A* 3:16440–16444
25. Nicollet C, Flura A, Vibhu V, Rougier A, Bassat JM, Grenier JC (2016) *Int J Hydrogen Energy* (in press)